Design and development of polynuclear ruthenium and platinum polypyridyl complexes in search of new anticancer agents

Schilden, Karlijn van der

Chapter 2

A paramagnetic dinuclear ruthenium(II)-ruthenium(III) complex: synthesis and strategy for ^{1}H NMR studies

Abstract – The terpyridyl-ruthenium(II) complex [(tpy)Ru(dtdeg)]Cl_2 (**1**) (tpy = 2,2':6',2"-terpyridine, dtdeg = bis[4'-(2,2':6',2"-terpyridyl)]-diethyleneglycolether) has been produced for the synthesis of the dinuclear ruthenium(II)-ruthenium(III) complex [(tpy)Ru(dtdeg)$RuCl_3$]Cl_2 (**2**). A straightforward strategy to fully characterize the paramagnetic species **2** by 1D and 2D ^{1}H NMR is reported. Complex **2** represents the first example of a paramagnetic ruthenium complex, which has been fully characterized using 1D NOE difference experiments. Plots of the observed chemical shifts *versus* the reciprocal temperatures indicate Curie behavior. Both contact and dipolar interactions are suggested to contribute to the hyperfine shift and nuclear relaxation. Delocalization of unpaired-spin density into the central pyridine ring, which is coordinated to the paramagnetic ruthenium(III) center, probably occurs by a spin polarization mechanism. The chemical shifts of the protons of the diamagnetic ruthenium(II) moiety are also affected by the unpaired electron. The influence is the smallest for the protons of the terminal terpyridine ligand.

2.1 Introduction

Polynuclear platinum complexes represent a new class of anticancer agents.[1] It is believed they can overcome resistance to the anticancer drug cisplatin, as they are capable of distinctive interactions with DNA, which is generally believed to be the ultimate target of platinum anticancer agents.[2] Ruthenium complexes are also known for their anticancer activity, and polynuclear derivatives are under study.[3] The synthesis of a series of dinuclear ruthenium complexes has been inspired by the mononuclear antimetastatic complex NAMI-A.[4] Dinuclear photoreactive ruthenium complexes have been designed, as it is thought that the greater size, charge and variation in shape increase DNA-binding affinity and specificity relative to mononuclear complexes.[5] The octahedral geometry of most ruthenium complexes is thought to impose unique interactions with biomolecules, which may cause a different anticancer profile from square-planar cisplatin.[6] Moreover, ruthenium(III) complexes may serve as prodrugs, which are activated by reduction *in vivo* to coordinate more rapidly to biomolecules.[3, 7] Selective tumor toxicity can be reached by the low oxygen content and the low pH in tumor cells, which are known to promote reduction.[3]

A challenge in the investigation of ruthenium(III) complexes is their characterization by ^{1}H NMR, because of the presence of an unpaired electron in the t_{2g} orbital of the low-spin d^5 ruthenium(III) ions. Paramagnetism induces hyperfine shifts of ^{1}H NMR signals and shortening of nuclear longitudinal (T_1) and transverse (T_2) relaxation times, which exclude characterization by standard ^{1}H NMR techniques used for diamagnetic molecules. Proton NMR studies of paramagnetic compounds have become increasingly useful in applications such as probing metalloprotein active-site structure and mechanism.[8, 9] However, for relatively small paramagnetic inorganic complexes, ^{1}H NMR has not been used intensively. It can be applied to small paramagnetic complexes in cases where the relaxation time of the unpaired electron is short enough, such that reasonably sharp ^{1}H NMR signals are observed. For low-spin ruthenium(III) complexes relatively short electronic relaxation rates of 10^{-11} s^{-1} have been reported,[10] which might make characterization by ^{1}H NMR possible.

In this Chapter, the synthesis and characterization of the ruthenium(II) complex $[(tpy)Ru(dtdeg)]Cl_2$ (**1**) (tpy = 2,2':6',2"-terpyridine, dtdeg = bis[4'-(2,2':6',2"-terpyridyl)]-diethyleneglycolether) and of the paramagnetic dinuclear ruthenium(II)-ruthenium(III) complex $[(tpy)Ru(dtdeg)RuCl_3]Cl_2$ (**2**, Figure 2.1) are presented. The synthesis of **2** has been based upon the cytotoxic and antitumor active complex[11] $[Ru(tpy)Cl_3]$, and the dinuclear derivative[12] $[Cl_3Ru(dtdeg)RuCl_3]$. These complexes have not been developed as possible anticancer drugs, because of their poor water solubility. The double positive charge of the bis(terpyridyl)-ruthenium(II) moiety of **2** is thought to increase water solubility. Moreover,

the positive charge of the ruthenium(II) moiety can direct **2** to the negatively charged DNA. Subsequently, the ruthenium(III) unit may coordinate to the DNA in a similar fashion[11, 13] as the parental mononuclear complex [Ru(tpy)Cl_3].

The ruthenium(III) moiety of **2** is paramagnetic, as is its mononuclear derivative. ^{1}H NMR studies have already been performed[12] on the latter and [Cl_3Ru(dtdeg)$RuCl_3$]. In this Chapter, a straightforward strategy is presented to fully characterize **2** by ^{1}H NMR experiments. It is shown for the first time that high-resolution ^{1}H 1D NOE NMR can be applied to low-spin ruthenium(III) complexes. To understand the relative weight of the different interactions between the unpaired electron and the nuclei on the hyperfine shift and nuclear relaxation, the ^{1}H NMR features displayed by **2** are discussed.

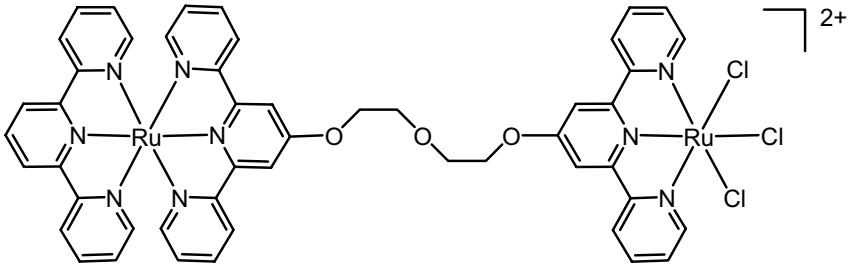

(**2**)

Figure 2.1 The dinuclear cationic ruthenium(II)-ruthenium(III) complex **2**.

2.2 Experimental section

2.2.1 General methods and starting materials

Elemental analyses on C, H and N were performed on a Perkin Elmer series II CHNS/O Analyzer 2400. Electrospray mass spectra were recorded on a Finnigan TSQ-quantum instrument with an electrospray interface (ESI). Hydrated $RuCl_3 \cdot xH_2O$ (x ~ 3) was used as received from Johnson & Matthey. The ligand tpy was obtained from Sigma. The ligand 4'-chloro-2,2':6',2"-terpyridine and the complex [Ru(tpy)Cl_3] have been synthesized according to known procedures.[14] The complex [(tpy)Ru(dtdeg)]Cl_2 has been synthesized according to a modified procedure for cationic $[Ru(L_1)(L_2)]^{2+}$ complexes in which L represents different tridentate heterocyclic ligands.[15] The acidic ruthenium(III) chloride solution and the ligand dtdeg have been synthesized[12] previously, but their synthesis will also be reported here for convenience (*vide infra*).

2.2.2 ^{1}H NMR measurements

^{1}H NMR spectra were mainly acquired on a Bruker DPX 300 spectrometer. 1D ^{1}H NOE difference spectra were measured on a Bruker DMX 600 spectrometer. Spectra were recorded in deuterated DMSO, and calibrated on the residual solvent peak at δ2.49 ppm. 1D ^{1}H spectra of **2** were obtained using a 100 ppm spectral width. Longitudinal relaxation times were measured by the standard inversion-recovery method, with 7 s relaxation delay and a spectral width of 100 ppm. Variable delays ranged from 50 μs to 500 ms to define the T1 values for the proton signals of the paramagnetic ruthenium(III) moiety, and from 100 ms to 5000 ms to define the T1 values for the proton signals of the diamagnetic ruthenium(II) moiety. Magnetization recovery was exponential within experimental error. T_2 values were estimated from the peak half-widths. The COSY spectrum was obtained by collecting 1024 F_2 x 1024 F_1 data points with a relaxation delay of 20 ms. 1D NOE experiments were carried out according to published procedures.[16] These procedures include a WEFT pulse sequence, which was not applied here. The irradiation time used for the 1D NOE experiment was 500 ms, and the number of scans 16384.

2.2.3 Syntheses

0.1 M ruthenium(III) solution:[12] $RuCl_3 \cdot xH_2O$ (1.20 g; ~ 5.0 mmol) was refluxed for 3 hours in 50 mL of a mixture of a 1 M HCl aqueous solution and EtOH (v:v = 1:1). The mixture was filtered and the filtrate was reduced *in vacuo* to 10 mL. A 1 M HCl aqueous solution (40 mL) was added to result in 50 mL of the required acidified ~ 0.1 M ruthenium(III) solution.

Dtdeg:[12] A mixture of 4'-chloro-2,2':6',2"-terpyridine (2.05 g; 7.6 mmol), diethyleneglycol (0.45 g; 4.2 mmol) and KOH (1.22 g; 21.7 mmol) was stirred in 185 mL of DMSO for 24 hours at 338 K, under a moisture-free atmosphere. 160 mL of water was added to the mixture at RT, which resulted in a white precipitate. The mixture was filtered and the residue was dried on air. The residue was dissolved in 350 mL of EtOH 98 % by reflux for ~ 1 hour. The desired product was precipitated upon cooling of the solution in an ice bath for 0.5 hour. The mixture was filtered and the residue was washed twice with a small amount (~ 5 mL) of ice cold EtOH 98 %. The product was dried on air. Yield: 1.75 g (80 %).

[(tpy)Ru(dtdeg)]Cl_2, (**1**): An excess of $AgBF_4$ (4.5 g; 23.1 mmol) was dissolved in 200 mL of acetone and filtered. [Ru(tpy)Cl_3] (0.800 g; 1.815 mmol) was added to the filtrate and the mixture was refluxed in the dark for 16 hours to remove the chloride ions from ruthenium. After filtration to remove precipitated AgCl, the filtrate was evaporated *in vacuo*, which

resulted in a green oil (~ 6 mL). The ligand dtdeg (1.700 g; 2.993 mmol) was added and the mixture was refluxed for 1.5 hours in 200 mL of DMF, which acted as the reducing agent. The reaction mixture was filtered and the red filtrate was evaporated *in vacuo*, which resulted in ~ 6 mL of an oil. To synthesize the chloride salt of the product, 75 mL of a saturated LiCl solution in EtOH was added to the oil. The desired product was obtained by precipitation with a large amount of acetone (~ 2 L). Complex **1** was separated from [(tpy)Ru(dtdeg)Ru(tpy)]Cl_4 by column chromatography on neutral alumina with acetone/MeOH/EtOH (v:v:v = 8:1:1). The first orange band contained pure product. Yield: 0.899 g (51 %). Elemental analysis (%) calculated for $C_{49}H_{39}Cl_2N_9O_3Ru{\cdot}6H_2O$ (water, originating from the used solvents, was used to fit the elemental analysis as the C/N ratio of the analysis corresponds to the structural formula of the complex): C 54.40, N 11.65, H 4.75. Found: C 54.51, N 11.96, H 4.95. ESI-MS: *m/z*: 452 [M^{2+}], 301 [M^{2+}+H^+]. ^{1}H NMR (300 MHz, DMSO, 298 K): δ = 8.61 (d, 2H; I33"), 7.99 (t, 2H; I44"), 7.48 (t, 2H; I55"), 8.67 (d, 2H; I66"), 8.03 (s, 2H; I3'5'), 4.51 (t, 2H; 1), 4.06 (t, 2H; 2), 8.87 (d, 2H; I'33"), 7.97 (t, 2H; I'44"), 7.21 (t, 2H; I'55"), 7.36 (d, 2H; I'66"), 8.87 (s, 2H; I'3'5'), 4.77 (t, 2H; 1'), 4.15 (t, 2H; 2'), 8.83 (d, 2H; II33"), 7.98 (t, 2H; II44"), 7.25 (t, 2H; II55"), 7,51 (d, 2H; II66"), 9.08 (d,2H; II3'5'), 8.48 ppm (t, 1H; II4').

[(tpy)Ru(dtdeg)RuCl$_3$]Cl$_2$, (**2**): **1** (0.190 g; 0.195 mmol) was dissolved in 60 mL of MeOH. At reflux temperature, 4 mL of the 0.1 M ruthenium(III) solution (0.4 mmol) was added to the solution. The mixture was refluxed for 3 hours and the resulting precipitate was filtered off at RT. The residue was dissolved in 1000 mL of hot MeOH and filtered to remove any insoluble species (probably ruthenium-oxo species). The filtrate was concentrated *in vacuo*, and the product was precipitated with diethyl ether. After filtration of the mixture, the residue was extensively washed with diethyl ether, which resulted in pure product. Yield: 0.082 g (36 %). Elemental analysis (%) calculated for $C_{49}H_{39}Cl_5N_9O_3Ru_2{\cdot}8H_2O{\cdot}0.5HCl$ (Besides water (*vide supra*), HCl was used to fit the elemental analysis, as the product precipitates from an acidic solution and an aqueous solution of the product is slightly acidic): C 43.80, N 9.38, H 4.16, Cl 14.51. Found: C 43.45, N 9.17, H 3.28, Cl 14.60. ^{1}H NMR (300 MHz, DMSO, 320 K): δ = –8.44 (s, 2H; I33"), 0.94 (s, 2H; I44"), –9.89 (s, 2H; I55"), –30.19 (s, 2H; I66"), 4.79 (s, 2H; I3'5'), 14.43 (s, 2H; 1), 4.12 (s, 2H; 2), 9.26 (s, 2H; I'33"), 8.09 (s, 2H; I'44"), 7.27 (s, 2H; I'55"), 7.82 (s, 2H; I'66"), 9.44 (s, 2H; I'3'5'), 5.26 (s, 2H; 1'), 4.41 (s, 2H; 2'), 8.90 (d, 2H; II33"), 8.09 (s, 2H; II44"), 7.27 (s, 2H; II55"), 7.53 (d, 2H; II66"), 9.15 (d,2H; II3'5'), 8.54 ppm (t, 1H; II4').

2.3 Results and discussion

2.3.1 Characterization of the diamagnetic precursor 1 by ^{1}H NMR spectroscopy

Complex **1** is water soluble. However, the ^{1}H NMR spectrum of **1** is shown in dmso-d_6 for comparison with **2** (Figure 2.2, assignments are reported in the experimental section). The appearance of four individual resonances in the region between 4 and 5 ppm for the linker protons 1, 2, 1' and 2' clearly indicates the presence of a non-symmetric species consisting of two different moieties. This is further confirmed by the fact that three sets of signals are recognized for the three inequivalent terpyridine ligands I, I' and II in the aromatic region by 2D ^{1}H NMR experiments (data not shown). Symmetry is displayed within each unit due to the occurrence of a C_2 symmetry axis, which is aligned along the linking diethylene glycolether chain and passes through the ruthenium center. Therefore, only half of the resonances for each terpyridine ligand are observed. The signals for the 66" protons have been identified by the small J value as compared to that of the 33" protons (~ 5 Hz *versus* ~ 9 Hz for the 66" and 33" protons, respectively). The terpyridine ligand II has been distinguished from the other terpyridine ligands by the signal for the II4' proton, since it is the only signal with a relative intensity of 1. The terpyridine ligands I and I' have been differentiated by the chemical shift of the 66" protons. The I'66" resonance is shifted upfield compared to the I66" signal, due to shielding of the former by the terpyridine ligand II.

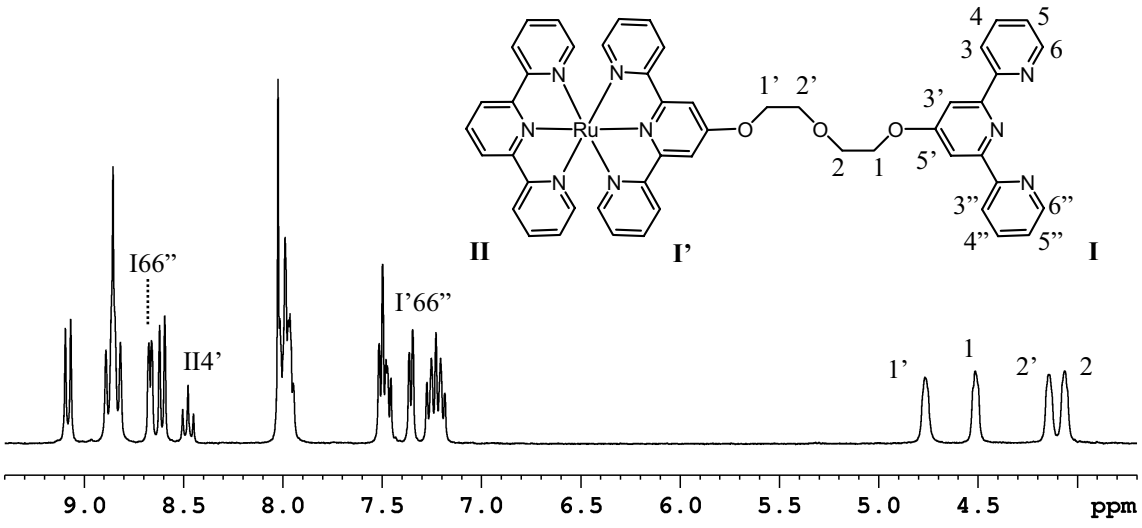

Figure 2.2 Schematic representation and 1D ^{1}H NMR spectrum of the cation of **1** in DMSO-d_6 at 298 K with some assignments. The numbering scheme given for terpyridine ligand I is also applicable to ligands I' and II.

2.3.2 ^{1}H NMR assignment strategy for the paramagnetic complex 2

Complex **2** is, like its precursor **1**, soluble in water. Since hydrolysis of **2** occurs in water, its 1D ^{1}H NMR spectrum is shown in dmso-d_6 (Figure 2.3). The spectrum has been acquired at 320 K. At this temperature, the "paramagnetic" signals, *i.e.* the resonances of the paramagnetic ruthenium(III) moiety, do not overlap. The effect of the unpaired electron of the paramagnetic species **2** is clearly recognized in the ^{1}H NMR spectrum. Most signals are observed in the normal diamagnetic envelope from 0 to 12 ppm, but some signals are greatly shifted upfield or downfield. The unpaired electron influences the magnetic field sensed by a proton, since a significant magnetic dipolar field is associated with the large magnetic moment of the unpaired electron, which is 658 times that of a proton.[8] The broadened and shifted resonances, which also display relatively short longitudinal relaxation times, have been classified as signals of protons of the paramagnetic trichlororuthenium(III) moiety. The signal at 4.79 ppm has also been established as a "paramagnetic" signal, since it exhibits short T_1 and T_2 values. Only 5 resonances are observed for the ruthenium(III) unit, because of the C_2 symmetry. The resonances appearing in the aromatic region have been assigned to the protons of the diamagnetic ruthenium(II) unit. This is fully consistent with the fact that the unpaired electron resides on the ruthenium(III) ion, and influences the nuclei closest to it the most. The striking similarities in chemical shift between the resonances for the terpyridine ligand I protons and the analogues resonances of the mononuclear parental complex [Ru(tpy)Cl$_3$] at the same temperature (Table 2.1), further confirm the assignment.

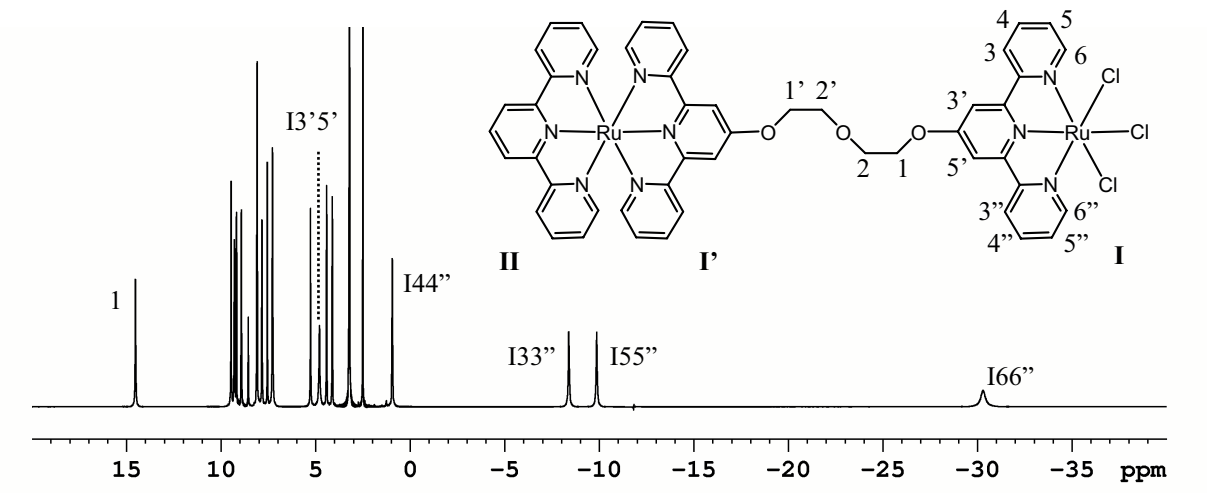

Figure 2.3 Schematic representation and 1D ^{1}H NMR spectrum of the cation of **2** in DMSO-d_6 at 320 K with some assignments. The numbering scheme given for terpyridine ligand I is also applicable to terpyridine ligands I' and II.

At 320 K, nine resonances, of which two have a relative intensity of 4, are observed in the aromatic region of the ^{1}H NMR spectrum of **2** (Figure 2.4). Thus, a total of eleven resonances are identified, which agrees with the structure and C_2 symmetry of the bis(terpyridyl)-ruthenium(II) moiety. The resonances of the terminal terpyridine ligand II appear as doublets and triplets, with exception of those that overlap with resonances of the I' terpyridine ligand. In contrast, all the resonances of the terpyridine ligand I' are significantly broadened. These signals also display relatively short longitudinal relaxation times. Fast relaxation rates result in a loss of magnetization during the various steps of the sequences of NMR experiments, which may cause a dramatic decrease in signal intensity.[8] For a 2D ^{1}H COSY NMR experiment of **2**, a relaxation delay of 20 ms resulted in a best signal-to-noise ratio in the aromatic region, as well as in the upfield region where most paramagnetic signals occur (*vide infra*). Since short acquisition times are a consequence of a short relaxation delay, a larger number of points (1024 in both dimensions) have been acquired in the same experimental time ensuing better resolution and signal intensity as well.

The resonances of the terpyridine ligand II have been assigned starting from its II4' proton, which displays a relative intensity of 1, using 2D ^{1}H COSY and NOESY experiments (data not shown). The I'3'5' resonance has been identified at 9.44 ppm, because no crosspeaks appear in the 2D COSY ^{1}H NMR. From the two signals at 9.26 and 7.81 ppm, the first most likely originates from the I'33" protons. The more upfield shifted signal at 7.81 ppm is expected to arise from the I'66" protons, since these protons are shielded by the terpyridine ligand II. A NOE between the I'3'5' and I'33" signals is not observed in 2D ^{1}H NOESY experiments, because the resonance positions are too close to resolve the crosspeak from the diagonal. In analogy with **1**, the signal at 5.26 ppm has been assigned to the linker protons 1'.

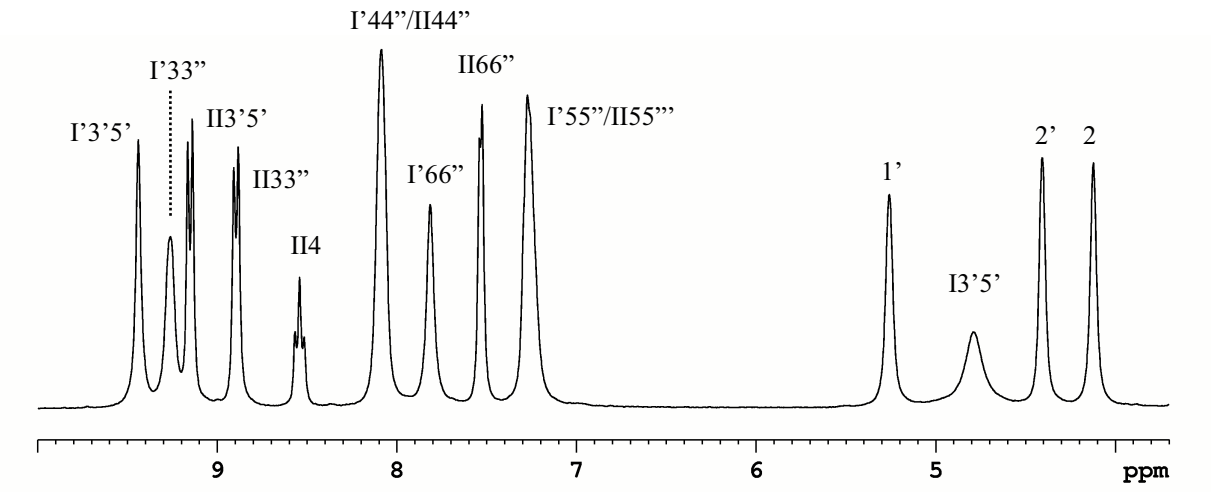

Figure 2.4 Part of the ^{1}H NMR spectrum of **2** in DMSO-d_6 at 320 K with assignments.

For the most "paramagnetic" signals of the paramagnetic species **2**, the success of a COSY experiment can be severely hampered by short transverse relaxation times T_2.[8] Indeed, the signal at –30.19 ppm appears to be too broad ($T_2 = 1/\pi$(fwh), in which fwh is the full width at half height) to show crosspeaks in a ^{1}H COSY NMR spectrum. The signal is expected to arise from the I66" protons, since these protons are closest to the paramagnetic ruthenium(III) ion. This signal is not only shifted and broadened the most, but also displays the shortest relaxation time T_1. The assumption is confirmed by 1D NOE experiments (*vide infra*).

In the upfield portion of the 2D COSY ^{1}H NMR spectrum a three-spins system is displayed (Figure 2.5). Taking into account the above assignment, the considered resonances can be assigned to the I33", I44" and I55" protons. The resonance at 0.94 ppm must arise from the I44" protons, as it displays crosspeaks to both resonances at –8.44 and –9.89 ppm. The latter resonances, corresponding to the I33" and I55" protons, cannot be distinguished from one another yet.

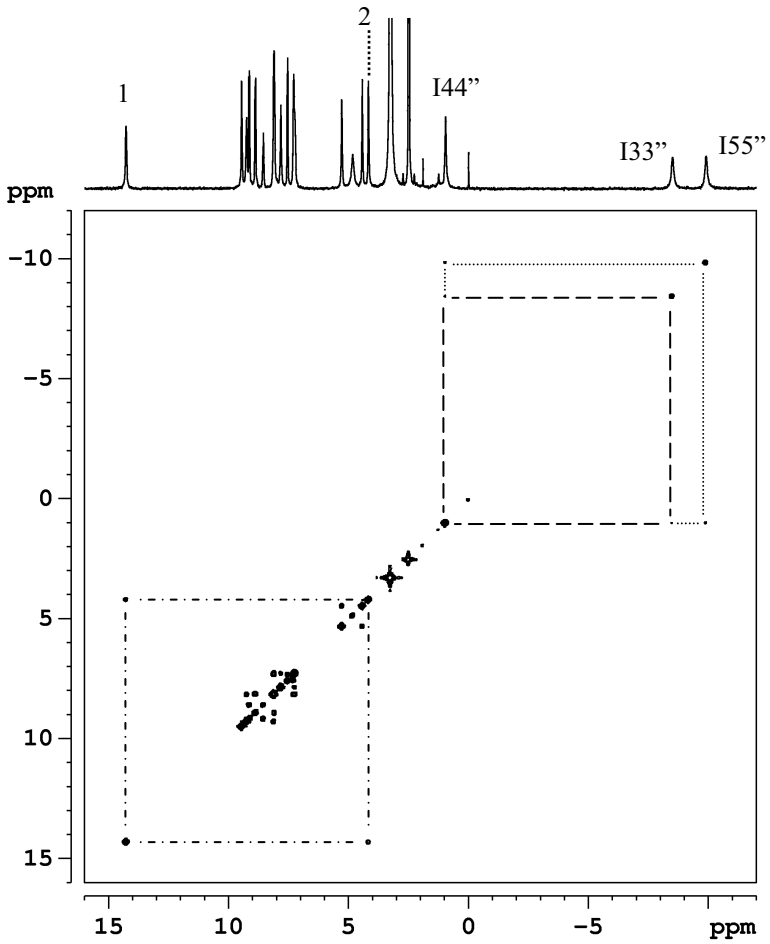

Figure 2.5 2D ^{1}H COSY NMR spectrum of **2** in DMSO-d_6 at 320 K with some assignments and crosspeaks indicated.

An additional spin-spin connectivity patterns involves the resonances at 14.43 and 4.12 ppm, which assigns these signals to the protons of the diethylene glycolether linker. The signal at 14.43 ppm is attributed to the 1 protons, *i.e.* the linker protons, which are closest to the ruthenium(III) ion.

Further assignments cannot be achieved without specific chemical substitution, which would require laborious syntheses, or interpretation of proton longitudinal relaxation times in correlation with distances between protons and the ruthenium(III) center. The latter are available from an earlier published[17] crystal structure of [Ru(tpy)Cl_3]. However, the distance to the metal determined for a proton using T_1 values may appear shorter than it really is when delocalized spin density is effective in relaxing the nucleus,[8] as may be the case for **2** (*vide infra)*. 1D steady-state NOE studies are likely to be the only resource for examining dipolar contacts of the protons close to the metal, since a maximum intensity of the NOE is obtained. The mixing time of a 2D NOESY experiment is relative short, and therefore the 2D NOESY response is less than that of a 1D NOE. 1D NOE difference experiments are often used to probe metalloprotein active-site structures, but have scarcely been used to study paramagnetic metal complexes. The NOE intensity for paramagnetic compounds is proportional to the rotational correlation time and inversely proportional to the longitudinal relaxation rate.[8] Therefore, the relatively small size and small T_1 values of paramagnetic complexes usually prevent the use of NOE techniques.

However, 1D NOE difference experiments have successfully been applied to characterize the paramagnetic ruthenium(III) complex **2**. Upon irradiation of the “paramagnetic” signal at 4.79 ppm, negative NOEs are displayed by the resonances at 14.43 and –8.44 ppm (upper spectrum, Figure 2.6). These signal enhancements clearly prove that the irradiated resonance originates from the I3’5’ protons, and that the resonances exhibiting NOEs arise from the linker 1 protons and the I33” protons, respectively. Using a 10 mM concentration and a great number of scans, irradiation of the I66” signal produces a signal enhancement at –9.89 ppm despite its short T_1 value. The NOE unambiguously confirms the assignment of the I66” protons, as well as that of the I55” protons, and completes successfully the full characterization of the paramagnetic species **2** by ^{1}H NMR. All “paramagnetic” signals have been irradiated and the observed NOEs confirm the assignments done by 2D COSY NMR. For the I3’5’ and I66” signals, NOEs are only observed upon irradiation of these resonances, but are not displayed upon irradiation of the I33” or 1 resonance, and the I55” signal, respectively. It has been recognized that larger NOEs occur upon saturation of the signal with a smaller T_1 value.[8]

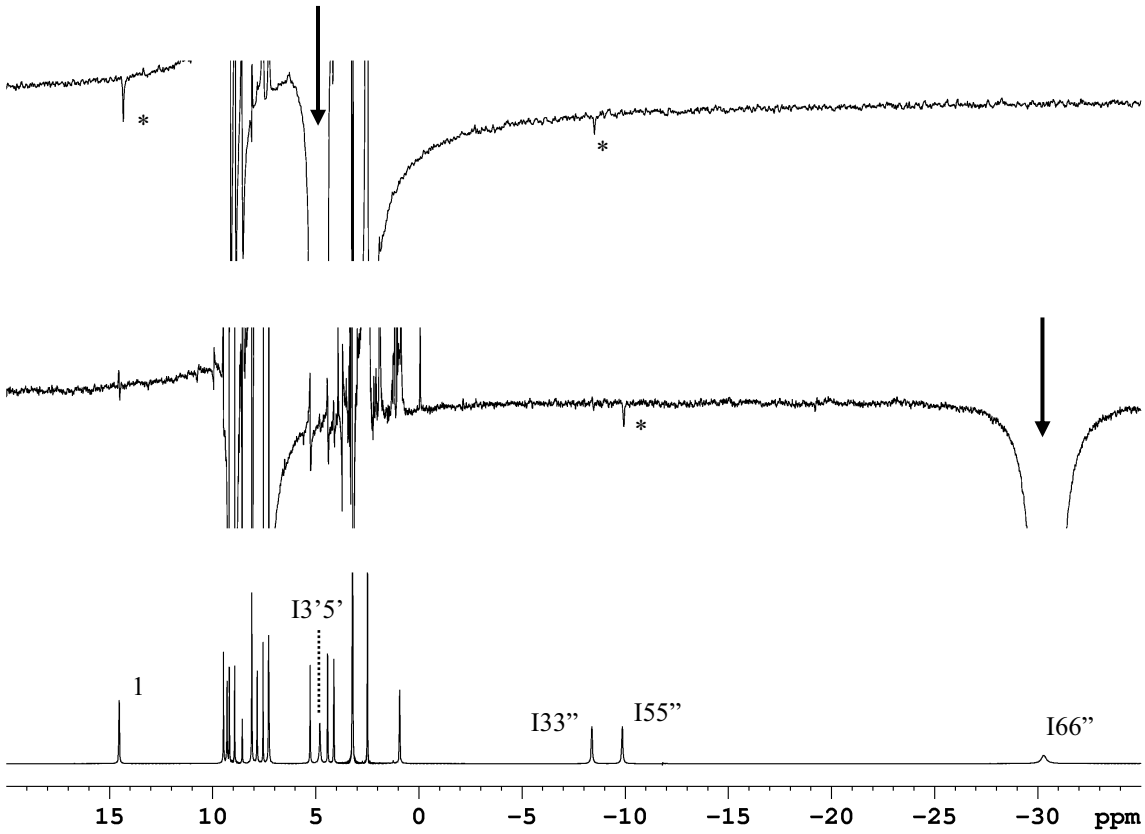

Figure 2.6 1D ^{1}H NOE difference NMR spectra (upper and center), and 1D ^{1}H NMR spectrum (bottom) of **2** in DMSO-d_6 at 320 K. Irradiated signals are indicated with an arrow. NOEs are indicated with an asterisk.

2.3.3 Temperature dependence of the chemical shift

Spectra of **2** were monitored by variable-temperature measurements over the temperature range 300 to 360 K (Figure 2.7). The chemical shifts of the paramagnetic protons are all temperature sensitive. They shift to the diamagnetic region upon an increase of the temperature.

The observed chemical shifts of the paramagnetic signals of **2** have been plotted against 1/T over the temperature range from 300 to 360 K (Figure 2.8). This Figure illustrates that the hyperfine shift linearly decreases upon a stepwise decrease of 1/T, which indicates Curie behavior. Curie's law (M = constant × H/T) states that magnetization (M) increases with an increase of the applied magnetic field (H), but decreases if the temperature increases.

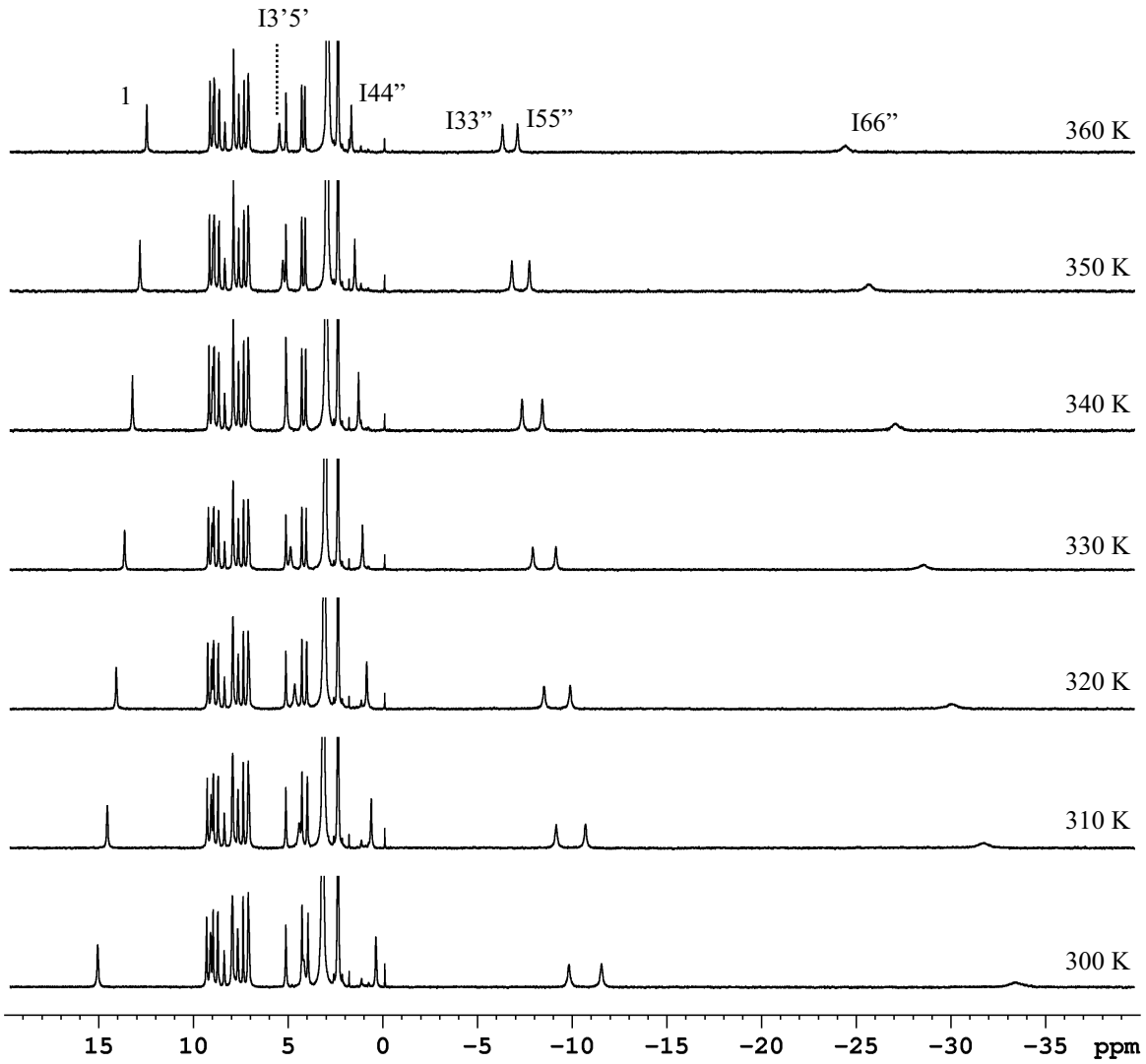

Figure 2.7 Variable temperature 1D ^{1}H NMR spectra for **2** in DMSO-d_6 in the temperature range from 300 to 360 K.

The equations (3) and (4) for the contact and dipolar shift, respectively (*vide infra*), indicate the linear dependency between the shift and the inverse of the temperature. From both equations it can be inferred that the observed chemical shift will approach the diamagnetic value as 1/T approaches zero. This behavior is also specified by the Curie law, which predicts zero magnetism at infinite temperatures. The intercepts obtained after extrapolation to infinite temperature for most of the signals differ only slightly from the expected diamagnetic shifts, which are in the aromatic region from 7 to 10 ppm. However, some intercepts deviate appreciably from their diamagnetic values. For example, the intercepts for I66" and I55" are 20.65 and 15.29 ppm, respectively. The reasons for a deviation from Curie behavior have not been studied here.

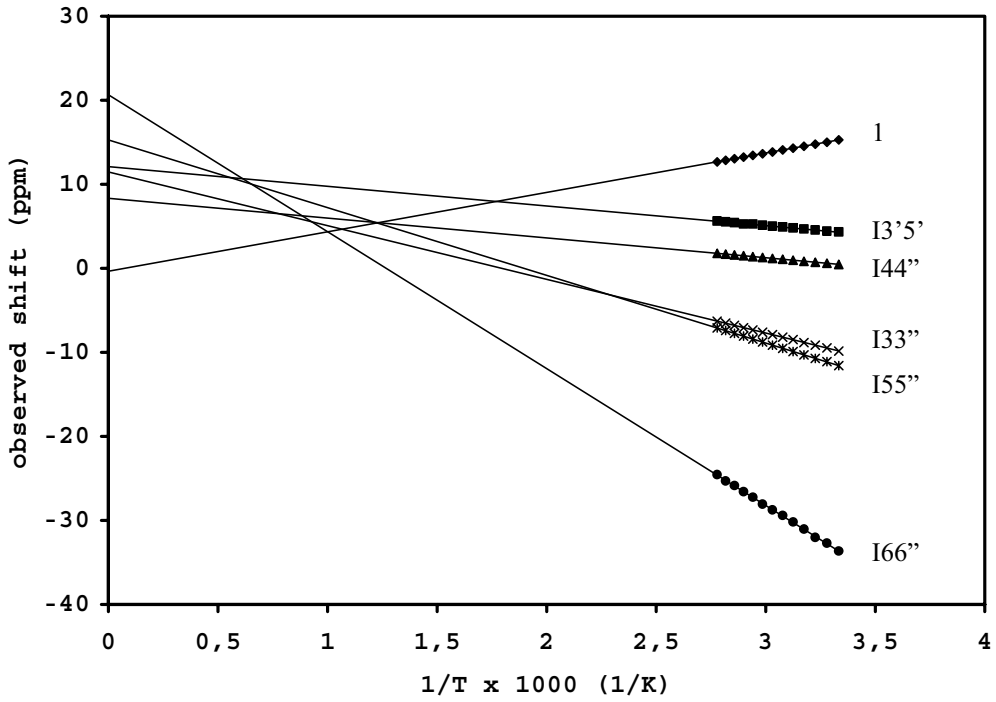

Figure 2.8 Plots of the chemical shift *versus* 1/T for **2**.

2.3.4 The hyperfine shift

For a proton of a paramagnetic species the observed ^{1}H chemical shift is different from its diamagnetic value because of the interaction between the proton nucleus and the unpaired electron, *i.e.* the hyperfine interaction (equation (1)). Contact (through bond) and dipolar (through space) couplings contribute to the hyperfine shift (equation (2)). The contact contribution to the hyperfine or isotropic shift is given[8] by equation (3), where A is the contact coupling constant, g_e is the free electron g-value, μ_B is the Bohr magneton, S is the spin quantum number of the spinning electron, $\hbar$ is Planck's constant divided by 2π, γ_I is the proton gyromagnetic ratio, k_B is the Boltzmann constant and T is the absolute temperature.
The contact shift is given by an additional magnetic field, which is generated at the nucleus by spin delocalization of the unpaired electron. The unpaired spin density is transmitted through antibonding molecular orbitals of the complex. Spin density may reach the nucleus by two different mechanisms. Direct spin delocalization occurs owing to the hydrogen contribution to the molecular orbitals that have unpaired electrons. The contribution to the hyperfine shift through this mechanism decreases rapidly as the number of chemical bonds between the metal and the resonating nucleus increases. Spin polarization arises, because the presence of an unpaired electron in a molecular orbital polarizes the paired electrons in a different molecular

orbital. Spin polarization can result in alternating positive and negative shifts in an aromatic system to yield zero spin density over the entire system per doubly occupied MO. Both the direct delocalization and polarization mechanism can occur through σ and π orbitals.

The dipolar or pseudocontact shift is given by equation (4), which is defined[8] for axially symmetric systems. The unpaired electron is considered to be localized on the metal in a paramagnetic complex. The shift is evaluated by expressing the principal molecular magnetic susceptibility values as a function of the principal g values, which holds when the spin multiplet ground state is well isolated from excited electronic states and zero-field splitting is negligible. μ_0 is the magnetic permeability of a vacuum, $g_{\parallel}$ and $g_{\perp}$ are the principal parallel and perpendicular g values, respectively, r is the metal-proton distance, and θ is the angle between the metal-nucleus vector $\boldsymbol{r}$ and the z component of the magnetic susceptibility tensor.

$$\delta_{observed} = \delta_{diamagnetic} + \delta_{hyperfine} \quad (1)$$

$$\delta_{hyperfine} = \delta_{contact} + \delta_{dipolar} \quad (2)$$

$$\delta_{contact} = \frac{A}{\hbar} \frac{g_e \mu_B S(S+1)}{3\gamma_I kT} \quad (3)$$

$$\delta_{dipolar} = \frac{\mu_0}{4\pi} \frac{\mu_B^2 S(S+1)}{9kT} (g_{\parallel}^2 - g_{\perp}^2) \frac{1}{r^3} (3\cos^2\theta - 1) \quad (4)$$

2.3.5 Contact and dipolar contributions to the chemical shifts of 2

The I33", I44", I55" and I66" protons of the trichlororuthenium(III) moiety of **2** display hyperfine shifts which agree with the metal-proton distances, as well as with the number of chemical bonds to the metal center. The protons closest to the paramagnetic ruthenium(III) ion (*i.e.* the I66" protons) display the largest hyperfine shift, whereas the protons furthest away from the unpaired electron (the I44" protons) show a relatively small hyperfine shift. These observations suggest that dipolar interactions or direct delocalization of spin density (or both) influences the shifts of these protons. In contrast, the I3'5' protons of the central pyridine ring of ligand I display a downfield shift with respect to the I33" and I55" signals, for which the metal-proton distances are approximately similar to that of the I3'5' protons. The shift of the I3'5' resonance agrees with[12] the signal of the same protons of the

mononuclear complex [Ru(tpy)Cl_3]. Interestingly, the 4' proton of the latter displays[12] a large upfield shift (–20.99 ppm) in comparison to its 44" signal, and the I44" resonance of **2**. Upfield shifts for *ortho* and *para* protons *versus* downfield shifts for *meta* protons have been observed before in six-membered π systems of paramagnetic molecules.[18] The shifts indicate that spin delocalization into the central pyridine ring of trichlororuthenium(III) terpyridyl complexes at least partly occurs by a spin polarization mechanism.

The unpaired electron of the low-spin ruthenium(III) ion occupies one of the t_{2g} orbitals, which have the correct symmetry for π bonding. Therefore, π delocalization of spin density is likely to occur. Once some unpaired spin density is present in a π system, it can spin-polarize the electrons of the C–H σ bond. The alternating chemical shifts of the pyridyl (Chapter 6) and phenyl[12] protons of [Ru(qpy)Cl_3] and [Ru(phtpy)Cl_3] (qpy = 4'-pyridyl-2,2':6'2"-terpyridine and phtpy = 4'-phenyl-2,2':6'2"-terpyridyl), support that spin polarization occurs in the central part of the terpyridine ligand.

Direct delocalization of spin density may occur into the outer pyridines of the terpyridine ligand I, because the ruthenium(III)-nitrogen coordination bonds are not orthogonal. The N-Ru-N" angle has been found[17] to be ~ 158.3(3)° for [Ru(tpy)Cl_3]. Therefore, overlap is expected between the ruthenium-nitrogen molecular orbitals and the t_{2g} metal orbital, which is located in the plane of the terpyridine ligand. Such overlap may cause transfer of unpaired spin density through σ bonds.

The relative weight of the dipolar or pseudocontact shift can be evaluated when both *g* values and structural information are available. For low-spin, d^5 metal complexes of octahedral symmetry EPR spectra can only be seen at temperatures close to liquid helium, because of the large spin-orbit coupling present. At the time of writing, no such measurements could be performed for **2**. However, EPR data of [Ru(tpy)Cl_3] have shown two g values (2.36 and 1.86), which indicates pseudo-axial symmetry. From the crystal structure of [Ru(tpy)Cl_3], which has previously been published,[17] metal-proton distances can be derived (Table 2.1). Hence, the contribution to the dipolar shift can be estimated. Using the known parameters of equation (4) gives $\delta_{dipolar} = 162.31/r^3 \, (g_{\parallel}^2 - g_{\perp}^2) \, (3 \cos^2 \theta - 1)$ ppm at 320 K (with *r* in Å). Taking into account that the geometric factor $(3 \cos^2 \theta - 1)$ can have a maximum value of 2, appreciable contributions to the pseudocontact shifts are possible. For example, the 66" protons, which are at ~ 3.1 Å from the ruthenium atom in [Ru(tpy)Cl_3], can have a maximum dipolar shift of 23 ppm. Large dipolar contributions to the shift have been reported for low-spin d^5 ruthenium.[19] Exact calculations of the dipolar shift require that the principal g directions are available. These can be obtained from single-crystal EPR measurements. The principal g directions may also be guessed from the symmetry of the molecule, which has not been achieved in this study.

The linker protons 1, which are relatively far from the paramagnetic center, show a relatively large downfield shift. Contact contributions to the shift through σ bonds are negligible, because of the large metal-proton distances. The shift may be due to a large contribution of the dipolar shift, or to a spin polarization mechanism, although it has been found for nickel(III) complexes that spin density cannot be transmitted through ethereal oxygen atoms.[20] Moreover, the chemical shifts of the terpyridine I' protons of the diamagnetic ruthenium(II) moiety differ significantly from those of the corresponding protons of the diamagnetic precursor **1** (*i.e.* 0.64 ppm for the I'3'5' signal; see experimental section). The ruthenium(II) moiety may closely approach the paramagnetic ruthenium(III) center, because of the high flexibility of the linker. This approach can result in dipolar interactions between the paramagnetic unit and the diamagnetic unit. However, the shifted and broadened signals of the protons of the diamagnetic unit can also originate from intermolecular interactions. Concentration-dependent ^{1}H NMR studies have not been performed to study these interactions. The fact that the protons of the terminal terpyridine ligand II are less affected by the paramagnetic metal center than the terpyridine I' signals, indicates a distance dependence of the influence of the unpaired electron, which supports intramolecular interactions are of importance.

2.3.6 Relaxation properties of 2

In Table 2.1, the chemical shifts and relaxation data are summarized for **2**. The shifts and T_1 and T_2 values of [Ru(tpy)Cl_3] are also reported here, as well as metal-proton distances, which have been derived from crystal structure data[17] of [Ru(tpy)Cl_3]. The I66" protons of **2**, which are closest to ruthenium, have a very short T_1 value (2.80 ms) and a broad line width (T_2 = 1.75 ms), whereas protons further away have longer T_1s and narrower line widths. This is expected because both T_1 and T_2 are dependent on r^{-6} due to dipolar relaxation contributions.[8] Thus, protons closer to the ruthenium center experience a stronger paramagnetic effect.

However, for the I3'5' protons the T_1 value is much shorter than that expected. Whereas the distance of the considered protons to the metal center is in between that of the I33" and I55" protons, T_1 is appreciably smaller (10.7 ms *versus* 17.7 and 28.5 ms, respectively). Delocalized π spin density onto the central pyridine clearly affects the relaxation of the I3'5' protons. In fact, the ratios between the T_1^{-1} values of all the different nuclei do not follow the ratios of the sixth power of the metal to nucleus distances. This indicates that also for the outer pyridines other contributions than dipolar interactions influence the relaxation.

Table 2.1 Chemical shifts and relaxation data for **2** and [Ru(tpy)Cl_3] at 320 K, 300 MHz , as well as metal-proton distances[17] for [Ru(tpy)Cl_3].

	2			**[Ru(tpy)Cl_3]**			
protons	δ_{obs} (ppm)	T_1 (ms)	T_2 (ms)	δ_{obs} (ppm)	T_1 (ms)	T_2 (ms)	$r_{Ru\text{-}H}$ (Å)
I66”	–30.19	2.80	1.75	–31.62	4.81	3.41	3.1
I55”	–9.89	28.6	9.2	–6.63	39.9	15.4	5.2
I44”	0.94	46.8	18.1	–2.48	54.5	20.3	5.7
I33”	–8.44	17.5	9.2	–7.87	31.6	15.8	4.9
I3’5’	4.79	10.7	8.8	5.90	20.3	15.4	5.1
I4’	–	–	–	–20.99	13.5	7.6	5.8
1	14.43	51.0	18.5	–	–	–	–
2	4.12	100.9	30.5	–	–	–	–

2.4 Concluding remarks

The preparations of the water-soluble ruthenium(II) complex [(tpy)Ru(dtdeg)]Cl_2 (**1**) and the water-soluble ruthenium(II)-ruthenium(III) complex [(tpy)Ru(dtdeg)$RuCl_3$]Cl_2 (**2**) are presented. Characterization of the paramagnetic complex **2** has been achieved in a straightforward manner by ^{1}H NMR spectroscopy. The data demonstrate that characterization of trichlororuthenium terpyridine complexes is feasible without laborious chemical substitution, elaborate examination of T_1 and T_2 relaxation times, or theoretical studies to calculate the different contributions to the chemical shift and nuclear relaxation rates. In fact complex **2** represents the first example of a paramagnetic ruthenium(III) complex, which has been fully characterized using 1D NOE difference experiments, despite relatively short relaxation times. The technique might be widely applicable to other paramagnetic inorganic complexes. Analysis of the chemical shift behavior *versus* temperature for the terpyridine I protons of the ruthenium(III) unit indicates Curie behavior. Both dipolar and contact interactions are suggested to contribute to the hyperfine shift of the different protons. Spin polarization is probably affecting the chemical shift of the I3’5’ protons. Comparison of T_1 and T_2 values with the metal-proton distances indicate that relaxation is determined by different unpaired-electron proton interactions. The chemical shifts of the protons of the diamagnetic ruthenium(II) unit are also influenced by the paramagnetic ruthenium(III) center. The shifts possibly originate from intramolecular interactions between the two moieties. Biological properties of **2** will be presented in Chapter 3.

2.5 References

[1] (a) Wheate, N. J.; Collins, J. G., *Coord. Chem. Rev.* **2003**, *241*, 133-145. (b) Reedijk, J., *Proc. Natl. Acad. Sci. U. S. A.* **2003**, *100*, 3611-3616.

[2] Reedijk, J., *Chem. Rev.* **1999**, *99*, 2499-2510.

[3] Clarke, M. J., *Coord. Chem. Rev.* **2003**, *236*, 209-233.

[4] (a) Iengo, E.; Mestroni, G.; Geremia, S.; Calligaris, M.; Alessio, E., *J. Chem. Soc.-Dalton Trans.* **1999**, 3361-3371. (b) Serli, B.; Iengo, E.; Gianferrara, T.; Zangrando, E.; Alessio, E., *Metal-Based Drugs* **2001**, *8*, 9-18.

[5] (a) Önfelt, B.; Lincoln, P.; Nordén, B., *J. Am. Chem. Soc.* **1999**, *121*, 10846-10847. (b) Wilhelmsson, L. M.; Westerlund, F.; Lincoln, P.; Nordén, B., *J. Am. Chem. Soc.* **2002**, *124*, 12092-12093. (c) Brodkorb, A.; Kirsch-De Mesmaeker, A.; Rutherford, T. J.; Keene, F. R., *Eur. J. Inorg. Chem.* **2001**, 2151-2160.

[6] Allardyce, C. S.; Dyson, P. J., *Platinum Metals Rev.* **2001**, *45*, 62-69.

[7] (a) Clarke, M. J.; Bitler, S.; Rennert, D.; Buchbinder, M.; Kelman, A. D., *J. Inorg. Biochem.* **1980**, *12*, 79-87. (b) Clarke, M. J.; Zhu, F. C.; Frasca, D. R., *Chem. Rev.* **1999**, *99*, 2511-2533.

[8] Bertini, I.; Luchinat, C., *NMR of paramagnetic substances, Coord. Chem. Rev. Vol. 150* (Ed.: Lever, A. B. P.), Elsevier, Amsterdam, **1996**.

[9] Bertini, I.; Luchinat, C.; Piccioli, M., in *Nuclear Magnetic Resonance of Biological Macromolecules, Pt B*, **2001**, *339*, 314-340.

[10] (a) Steiner, U. E.; Serebrennikov, Y. A., *J. Chem. Phys.* **1994**, *100*, 7503-7507. (b) Serebrennikov, Y. A.; Steiner, U. E., *J. Chem. Phys.* **1994**, *100*, 7508-7514.

[11] Nováková, O.; Kašpárková, J.; Vrána, O.; Van Vliet, P. M.; Reedijk, J.; Brabec, V., *Biochemistry* **1995**, *34*, 12369-12378.

[12] Velders, A. H., Ph.D. thesis, Leiden University (Leiden), **2000**.

[13] Van Vliet, P. M.; Toekimin, S. M. S.; Haasnoot, J. G.; Reedijk, J.; Nováková, O.; Vrána, O.; Brabec, V., *Inorg. Chim. Acta* **1995**, *231*, 57-64.

[14] (a) Potts, K. T.; Konwar, D., *J. Org. Chem.* **1991**, *56*, 4815-4816. (b) Holbrey, J. D.; Tiddy, G. J. T.; Bruce, D. W., *J. Chem. Soc.- Dalton Trans.* **1995**, 1769. (c) Constable, E. C.; Ward, M. D., *J. Chem. Soc.- Dalton Trans.* **1990**, 1405. (d) Sullivan, B. P.; Calvert, J. M.; Meyer, T. J., *Inorg. Chem.* **1980**, *19*, 1404-1407.

[15] Sauvage, J. P.; Collin, J. P.; Chambron, J. C.; Guillerez, S.; Coudret, C.; Balzani, V.; Barigelletti, F.; Decola, L.; Flamigni, L., *Chem. Rev.* **1994**, *94*, 993-1019.

[16] (a) Dugad, L. B.; Lamar, G. N.; Banci, L.; Bertini, I., *Biochemistry* **1990**, *29*, 2263-2271. (b) Banci, L.; Bertini, I.; Luchinat, C.; Piccioli, M.; Scozzafava, A.; Turano, P., *Inorg. Chem.* **1989**, *28*, 4650-4656.

[17] Laurent, F.; Plantalech, E.; Donnadieu, B.; Jimenez, A.; Hernandez, F.; Martinez-Ripoll, M.; Biner, M.; Llobet, A., *Polyhedron* **1999**, *18*, 3321-3331.

[18] (a) Ming, L. J.; Banci, L.; Luchinat, C.; Bertini, I.; Valentine, J. S., *Inorg. Chem.* **1988**, *27*, 4458-4463. (b) Lamar, G. N., *J. Am. Chem. Soc.* **1965**, *87*, 3567-&.

[19] Clarke, M. J.; Bailey, V. M.; Doan, P. E.; Hiller, C. D.; LaChance-Galang, K. J.; Daghlian, H.; Mandal, S.; Bastos, C. M.; Lang, D., *Inorg. Chem.* **1996**, *35*, 4896-4903.

[20] (a) Eaton, D. R.; Josey, A. D.; Benson, R. E.; Phillips, W. D.; Cairns, T. L., *J. Am. Chem. Soc.* **1962**, *84*, 4100. (b) Eaton, D. R.; Josey, A. D.; Phillips, W. D.; Benson, R. E., *J. Chem. Phys.* **1962**, *37*, 347.